Water Conservation Science and Engineering (2021) 6:191–200
https://doi.org/10.1007/s41101-021-00113-0

ORIGINAL PAPER

# Study on Water Flow Capacity and Related Parameters of Spillway Gate of Orifice Outflow Dam

**Yaxia Lu[1] · Xushu Sun[2]**

Received: 5 July 2021 / Revised: 11 August 2021 / Accepted: 11 August 2021 / Published online: 3 September 2021


## Abstract

The largest part of the water control project belongs to the low-head riverbed floodgate project, and its discharge capacity can be accurately determined in design, which can avoid the inundation of the upstream fertile land and at the same time achieve the purpose of reducing the scale of flood discharge structures and saving project investment. In this paper, the influence of different height difference between the dam floor and the upstream and downstream riverbeds on the discharge capacity is studied through the model test of the discharge capacity and its related parameters of the spillway gate of the orifice outflow dam, and the three-dimensional flow field of the discharge flow of the spillway gate is numerically simulated by FLUENT commercial software. The Reynolds equation is closed by using the standard $K$-ε turbulence numerical model, and the free liquid level is tracked by using the volume of fluid (VOF) method. The tetrahedral unstructured grid is used to divide the grid, and the calculation results of the discharge capacity, flow pattern, water level elevation, velocity field, and pressure field of the floodgate are obtained. Compared with the observation results of the model test, they are in good agreement, which shows that the model used in the numerical simulation is reasonable and the method is correct.

**Keywords** Orifice outflow dam · Water flows through · Flood gate · Related parameters

## Introduction

In the water conservancy and hydropower project, the discharge structure is a hydraulic structure used to discharge the excess water, floating objects, sediment, and ice in the reservoir. The discharge structure plays a vital role in the safe and smooth operation of the reservoir. Flood discharge capacity is an important data basis in building shape design [1]. When the designed discharge of the discharge structure is less than the actual discharge of the project, it will lead to flooding of the fertile land downstream of the hub and major property losses. When the designed discharge of the discharge structure is larger than the actual discharge of the project, resources will be wasted in the project construction. Therefore, it is crucial to accurately determine the discharge capacity of flood discharge structures in the design and research of hydraulic engineering.

As early as 1950s, someone established the mathematical model theory, but it was not put into use immediately. Later, with the advent of computers, numerical models began to be used in hydraulics research. Literature [1] and literature [2] use some new methods, such as the control volume method of non-orthogonal grid and the turbulence model of $k$-ε equation, to solve the N-S equation of two-dimensional time average, and discuss the treatment of the free water surface with unknown position. Literature [3, 4] use volume of fluid (VOF) mathematical model of water–gas two-phase flow to carry out two-dimensional numerical simulation of surface hole flood discharge and compare the experimental values and find that they are very consistent, thus finding a new solution for solving such problems and obtaining more information. Literature [5] analyzes that the flow characteristics of submerged jet in plunge pool are different from those of submerged free jet due to the constraint of solid boundary and discusses the significance of applying numerical simulation method to study this problem. Literature [6] simulates the discharge capacity curve of spillway by FLUENT software. The pressure value of the center line of the bottom

✉ Xushu Sun
s3h5xx@yeah.net

[1] Journal Office of China Three Gorges University, Yichang 443002, Hubei, China

[2] College of Hydraulic and Environmental Engineering, China Three Gorges University, No. 8, College Road, Xiling District, Yichang 443002, Hubei, China

plate is obtained by post-processing software and compared with the data measured by hydraulic experiment, it is concluded that the calculated maximum and minimum pressure values are basically consistent with the test data at the same position (Literature [7, 8] and Literature [9]). Based on the 1: 50 model test results of a power station inlet, the flow field at the inlet is simulated and calculated, and the influence of inflow and complex terrain boundary on the flow pattern at the inlet is studied. Literature [10] uses FLUENT software to simulate the hydraulic jump behind the gate, uses standard $K\sim\varepsilon$ turbulence model to close Reynolds equation, and uses VOF method to track the free water surface. Finally, the numerical simulation results are in good agreement with the measured results of model test, which shows that FLUENT software can simulate turbulent flow well.

Based on the research on the water flow capacity of spillway gate of orifice outflow dam at home and abroad, it mainly focuses on the study of high-head bottom hole and lacks the corresponding systematic analysis of the flow pattern in the outlet of diversion bottom hole and its downstream open channel. This paper is based on the actual hydraulic physical model, aiming at solving the practical problems of hydraulic engineering. With the help of FLUENT software, the author carried out the three-dimensional numerical simulation of the overflow flow field of the spillway gate of the orifice outflow dam. After we compared it with the hydraulic model test results, we began to verify the reliability and feasibility of the numerical simulation and provided constructive guidance for us to carry out this kind of work in the future.

## Research Technique

Computational fluid dynamic (CFD), which integrates many disciplines such as computational mathematics, computer technology, physical model, and CAD visualization, has become an interdisciplinary science. With the rapid development of computer technology and continuous improvement of numerical methods, more and more researchers pay attention to the numerical simulation of turbulence. Turbulence, also known as turbulence, is a common highly nonlinear complex flow in nature, and its characteristics play an important role in engineering. In this section, the commercial software FLUENT is used to simulate the three-dimensional flow field of the spillway sluice. The VOF method is used to track the free liquid surface, and tetrahedral unstructured grid is used for grid division.

### Numerical Simulation of Turbulence

Direct numerical simulation and indirect numerical simulation are two major methods of turbulent numerical simulation. Direct numerical simulation method is abbreviated as DNS method. That is to say, solving the governing equation of instantaneous turbulence directly, without any simplified or approximate treatment of turbulent flow, can theoretically obtain relatively accurate calculation results [11, 12], which is the greatest advantage of this method. The indirect numerical simulation method, that is, by trying to approximate or simplify the turbulent flow to some extent, can be divided into statistical average method, large eddy simulation, and Reynolds average method. Statistical average theory mainly involves the motion of small-scale vortices, which is not widely used in engineering. Large eddy simulation uses instantaneous N-S equation to directly simulate large-scale eddy, while small-scale eddy is closed and approximated by model, so large eddy simulation requires higher computer memory and CPU speed.

Reynolds average method is an indirect numerical simulation method widely used in engineering. Its core is not to directly solve the instantaneous Navier–Stokes equation, but to find a way to solve the time-averaged Reynolds equation [13]. In this way, it can not only avoid the problem of large amount of calculation of DNS method, but also achieve good results in practical engineering application. Figure 1 is the classification diagram of Reynolds average method.

Reynolds stress model and eddy viscosity model are two commonly used turbulence models. In Reynolds stress model, the Reynolds stress equation is established directly, and the time-averaged continuous equation and the time-averaged N-S equation are solved simultaneously. According to the form of Reynolds stress equation, Reynolds stress model includes Reynolds stress equation model and algebraic stress equation model.

In the eddy viscosity model, Reynolds stress term is not directly dealt with, but viscous eddy coefficient is introduced, and turbulent stress is expressed as a function of eddy viscosity coefficient. Determining eddy viscosity coefficient is the key of the whole calculation. The eddy viscosity coefficient comes from the eddy viscosity hypothesis proposed by Boussinesq, which establishes the relationship between Reynolds stress and average velocity gradient [14, 15], namely:

$$-\overline{\rho u_i u_j} = u_i\left[\frac{\partial u_i}{\partial x_j}+\frac{\partial u_j}{\partial x_i}\right]-\frac{2}{3}\left\{\rho k+\mu_i\frac{\partial u_i}{\partial x_i}\right\}\delta_{ij} \tag{1}$$

In the formula, $\mu_i$ represents turbulent viscosity, $u_i$ represents time-averaged velocity, $\delta_{ij}$ is the symbol "Kronecker delta" (when $i$ is equal to $j$, $\delta_{ij}=1$; when $i$ is not equal to $j$, $\delta_{ij}=0$), and $k$ represents turbulent kinetic energy:

$$k=\frac{\overline{u_i u_j}}{2}=\frac{1}{2}\left(\overline{u_i^2}+\overline{v^2}+\overline{u_j^2}\right) \tag{2}$$

Turbulent viscosity $\mu_t$ is a spatial coordinate function, not a physical parameter, and its size depends on the flow

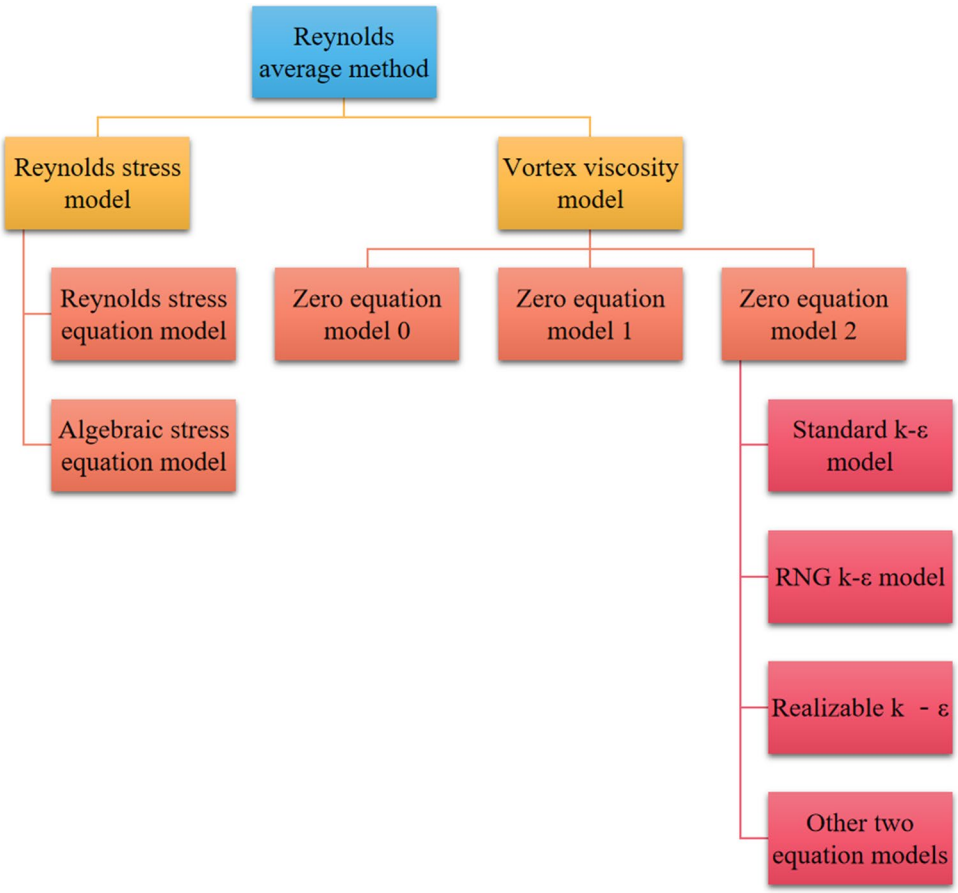


**Fig. 1** Classification diagram of Reynolds average method

state. How to determine turbulent viscosity $\mu_t$ is the key to calculate turbulent flow. Vortex viscosity model is a relational expression that combines turbulent viscosity $\mu_t$ with time-averaged parameters. According to the number of differential equations to determine $\mu_t$, the eddy viscosity model can be divided into zero equation model, one equation model and two-equation model.

## VOF Model

VOF method was proposed by Hirt and Nichols in 1981 [16]. It determines the free surface and tracks the change of fluid by studying the ratio function $F$ of fluid and mesh volume in the mesh unit. If $F=0$, it means that the unit is all occupied by the specified first phase fluid; if $F=1$, the unit is completely occupied by the designated second phase fluid, and there is no first phase fluid; when $0<F<1$, the unit is called interface unit, which has both the first phase fluid and the second phase fluid.

In VOF model, it is considered that water and gas have the same velocity field and pressure field, so the water–gas two-phase flow can be described by the same set of equations:

$$\rho = F_{\rho w} + (1-F)\rho_a \tag{3}$$

$$\mu = F_{\mu_w} + (1-F)\mu_a \tag{4}$$

in which $\rho_w, \rho_a$ is the density of water and air and $\mu_w, \mu_a$ is the molecular viscosity coefficient of water and air, respectively.

## Boundary Conditions and Convergence Judgment

The mathematical and physical conditions that flow field variables should meet on the calculation boundary become boundary conditions, which are an indispensable part of numerical simulation. Whether the boundary conditions are correct or not directly affects whether the program can be carried out normally and whether the calculation results are correct. The determination of boundary conditions includes two aspects: given accurate boundary shape and accurate boundary conditions. When dealing with these two problems, the flow mechanism will be involved, and it will be very difficult to solve them.

Basic boundary conditions include [17, 18] inlet boundary, outlet boundary, wall boundary condition, symmetric

boundary condition, and periodic boundary condition. In the three-dimensional numerical simulation of the spillway gate of the orifice outflow dam, only three boundary conditions are involved: the inlet boundary, the outlet boundary, and the wall boundary conditions, and only these three boundary conditions are introduced below:

(1) Import boundary condition

Velocity inlet boundary condition and pressure inlet boundary condition are the most commonly used inlet boundary conditions. The boundary condition of velocity inlet, that is, the magnitude and direction of velocity on the inlet section, is known, which can only be given by physical model. In this paper, the pressure inlet boundary condition is used to define the pressure of the flow inlet and the parameters of other scalar characteristics of the flow. Parameters such as absolute pressure, turbulent kinetic energy, and dissipation rate should be considered when using pressure inlet boundary conditions. Therefore, the boundary conditions are described as follows:

Setting of reference pressure

In the process of numerical simulation, the actual pressure value is relative to the inlet pressure, not absolute value. Therefore, it is necessary to set the pressure value at the inlet to solve the pressure value at other points. Sometimes, in order to reduce the digital truncation error, the reference pressure point is deliberately raised or lowered, so that the calculated pressure fields in other places are consistent with the magnitude of the whole numerical calculation. In this paper, the highest point at the entrance of the reservoir area is selected as the pressure reference point, and the pressure value is the standard atmospheric pressure.

Estimated values of $k$ and $\varepsilon$

In this paper, the standard $k-\varepsilon$ model is used to close the turbulence model. It is necessary to give the estimated values of turbulent kinetic energy $k$ and turbulent kinetic energy dissipation rate $\varepsilon$ at the boundary of the port and choose the following empirical formula to determine these two parameters [19]:

$$k = 0.00317\mu^2 \tag{5}$$

$$\varepsilon = \frac{k^{\frac{3}{2}}}{0.4L} \tag{6}$$

In the formula, $\mu$ takes the average flow velocity at the inlet section, $L$ is the characteristic length of turbulent flow, and the hydraulic radius $R$ is used instead in calculation.

(2)Exit boundary condition

Outlet boundary refers to the setting of flow parameters at the outlet boundary. The outlet is generally located far enough away from geometric disturbance. Turbulence is fully developed and changes little along the fluid flow direction. The cross section perpendicular to the flow direction can be selected. In this paper, the boundary condition of pressure outlet is adopted, that is, static pressure is set at the outlet position, and the outlet pressure is considered as atmospheric pressure.

(3)Boundary condition of solid wall

The wall is used to distinguish between fluid and solid areas. In viscous flow, the default boundary condition at the wall is no slip boundary condition, but a "slip" wall can be simulated by specifying shear, or a tangential velocity component can be specified according to the rotation or translation of the wall boundary region. Compared with the low Re number model, the wall function method is more efficient and practical in engineering [20]. When using $k-\varepsilon$ model with low Re number, because the physical quantity changes greatly in the wall area (viscous bottom layer and transition layer), it is necessary to use fine grid to divide the calculation area, which greatly increases the calculation cost. Therefore, this paper adopts the wall function method to deal with the flow near the wall.

## Analysis of Experimental Results

### Influence of Height Difference on Discharge Capacity

According to the test data, the relationship curves between discharge coefficients $m$ and $P_1/H_0$ with different $P_1$ values are drawn with $P_1$ as the parameter (Fig. 2).

It can be seen from Fig. 2 that, within the test flow range, under the condition of the same bed surface elevation, that is, the $P_1$ value is unchanged, the flow coefficient $m$ increases with the decrease of $P_1/H_0$ (that is, the larger the relative head $H_0/P_1$). For different $P_1$ values, the curves with relatively large $P_1$ values in the curve cluster are all located above the relatively small $P_1$ values, which indicates that the lower the upstream riverbed, that is, the larger the $P_1$ value (which can be described by the relative height difference $P_1/L$), the stronger the flow capacity of the gate hole, the more adequate the streamline development, and the larger the discharge coefficient $m$.

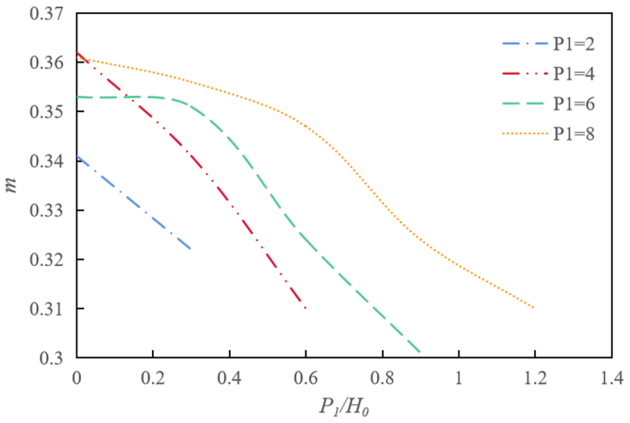


**Fig. 2** The relationship between flow coefficient $m$ and $P_1/H_0$

## Flooding Degree Affects Discharge Capacity

See Fig. 3 for water flow pattern and velocity distribution in the reservoir area and the downstream of the floodplain under check, design, flood once in 30 years, and other working conditions. It can be seen from the figures and photographs that the flow patterns of the reservoir areas under three working conditions are basically similar. After entering the reservoir area, the water flows from the center to the left, with rapid flow (the maximum velocity in the reservoir area is over 5 m/s), large water surface waves, and unstable and smooth flow pattern (see Fig. 3b and Fig. 3c). Before entering the dam, the water flow forms a top impact on the auxiliary dam on the left bank and produces backflow (the maximum backflow velocity is about 0.3 m/s), so the water level on the left bank before the dam is higher than that on the right bank.

The water retaining structures of flood control projects mostly adopt the design scheme of full sluice or flood gate + overflow dam. In any layout mode, in order to reduce the discharge requirements and reduce the project cost, it is necessary to reduce the number of sluice holes or the discharge width [21]. Because of the lower gate floor and the lower weir crest elevation, the flood discharge and submergence degree of the low gate hub are large, and it is difficult to accurately calculate its discharge capacity. Therefore, there is some error in the formula of the weir flow with wide crest, which is analyzed as follows.

Weir flow formula:

$$Q = \sigma_s m B \sqrt{2g} H_0^{3/2} \tag{7}$$

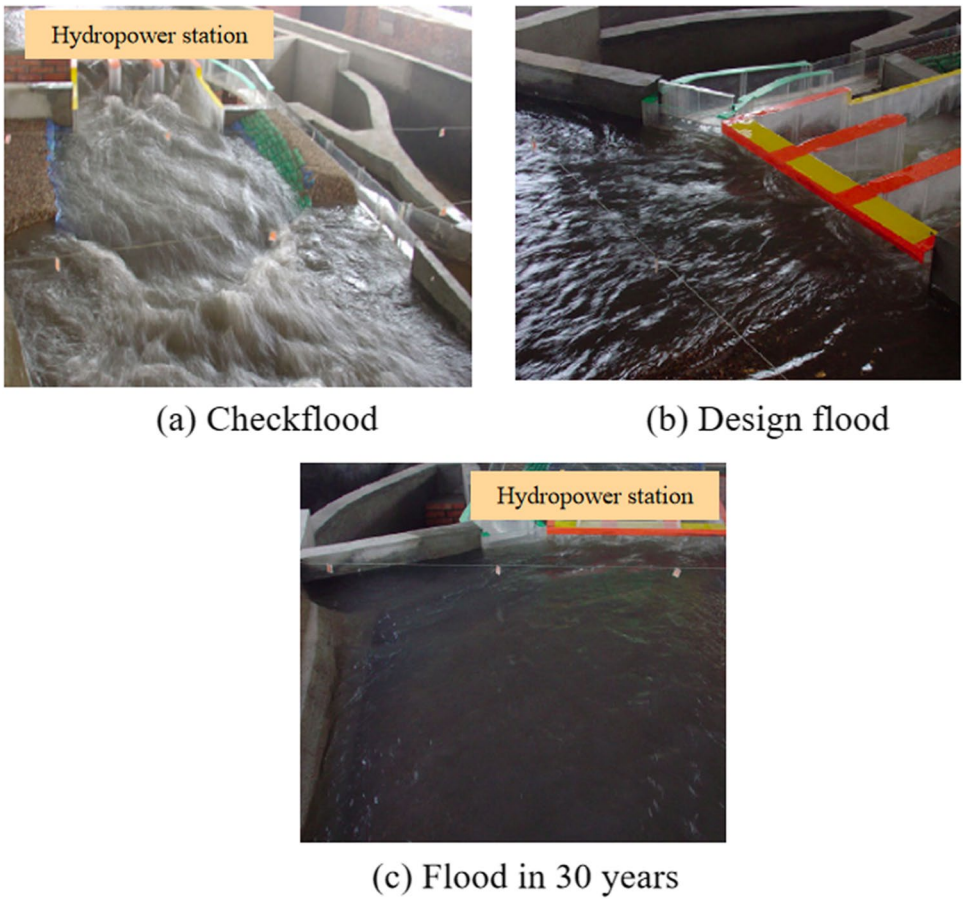


**Fig. 3** Energy dissipation and scour prevention test downstream of the hub

$$\sigma_s = f\left(\frac{h_s}{H_0}\right) \tag{8}$$

$$H_0 = H + \frac{v_0^2}{2g} \tag{9}$$

Among them,

$Q$ Flow rate ($m^3/s$);
$B$ Width of weir (m);
$h_s$ The water depth exceeding the weir crest (m);
$H$ Head on weir (m);
$H_0$ Total water head on weir (m);
$m$ Flow coefficient;
$\sigma_s$ Submerged coefficient.

By drawing the relationship curve between inundation coefficient $\sigma_s$ and inundation degree $h_s/H_0$ (Fig. 4), it can be seen that with the increasing inundation degree, the inundation coefficient decreases, and the curve changes smoothly at the beginning. However, when $h_s/H_0$ exceeds 0.82, the curve gradually becomes steep, the submergence coefficient drops rapidly, and the value becomes more and more unstable. Other assumed conditions are unchanged, so that the

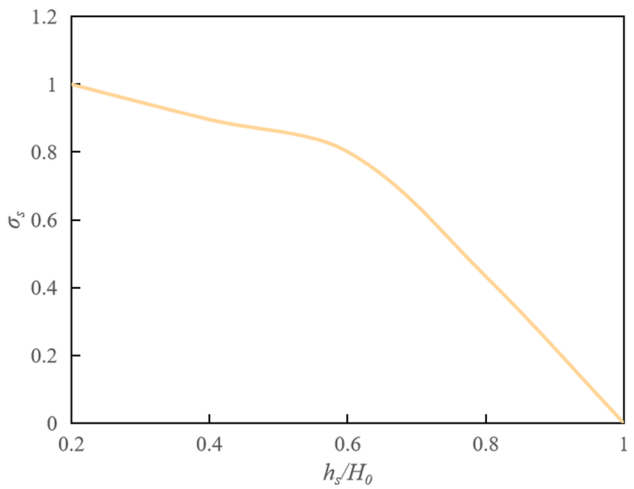


**Fig. 4** Relationship between submergence coefficient $\sigma_s$ and submergence degree $h_s/H_0$

possible error of $\sigma_s$ is $\Delta\sigma_s$, and the relative error between discharge and water level variable can be deduced from weir flow formula (7):

$$\left|\frac{\Delta Q}{Q}\right| = \left|\frac{(Q+\Delta Q)-Q}{Q}\right| = \left|\frac{(\sigma_s+\Delta\sigma_s)mB\sqrt{2g}H_0^{3/2} - \sigma_s mB\sqrt{2g}H_0^{3/2}}{\sigma_s mB\sqrt{2g}H_0^{3/2}}\right| = \left|\frac{\Delta\sigma_s}{\sigma_s}\right| \tag{10}$$

$$\left|\frac{\Delta H_0}{H_0}\right| = \left|\frac{(H_0+\Delta H_0)}{H_0}\right| = \left|\frac{\left(\frac{Q}{(\sigma_s+\Delta\sigma_s)mB\sqrt{2g}}\right)^{2/3} - \left(\frac{Q}{\sigma_s mB\sqrt{2g}}\right)^{2/3}}{\left(\frac{Q}{\sigma_s mB\sqrt{2g}}\right)^{2/3}}\right| = \left|\left(\frac{1}{1+\frac{\Delta\sigma_s}{\sigma_s}}\right) - 1\right| \tag{11}$$

When the other assumptions remain unchanged and the submergence error is $\Delta h_s/H_0 = 0.02$, the relative values of submergence coefficient, discharge, and water level error can be obtained according to Fig. 4 and Eqs. (10) and (11). According to Table 1, after the submergence degree $h_s/H_0$ of flood gate or overflow dam exceeds 0.86, the value of submergence coefficient decreases rapidly, and when there is a slight deviation in the calculation process of submergence degree, the change range of submergence coefficient is larger, so the error of water level in front of dam under the given discharge calculated by formula (7) is larger.

According to the calculation of weir flow formula and the relationship between inundation coefficient $\sigma_s$ and inundation degree $h_s/H_0$, it is shown that the calculation error of flood discharge capacity of floodgates with higher inundation degree is large, and the model test must be used to further determine the accuracy of the error, so as to achieve the ideal goal of reasonably determining the number of floodgates and overflow width.

## Cross-Section Velocity of Spillway Gate

The free water surface is extremely important for the structural design of flood gates and the operation of reservoirs. When the water flows down, it will be accompanied by atomization. The water surface is a transition interface from water to gas, and the position of the water surface is generally difficult to be clearly defined. During the hydraulic model test, the water surface position is clear, with little change, and can be measured, which is an obvious difference between prototype observation and hydraulic model test [22]. In the hydraulic model test, the velocity of the

**Table 1** Table of relative values of submergence coefficient, discharge, and head error on weir

| $h_s/H_0$ | 0.30 | 0.40 | 0.50 | 0.60 | 0.70 | 0.80 | 0.90 | 1.0 |
|---|---|---|---|---|---|---|---|---|
| $\Delta h_s/H_0$ | 0.01 | 0.01 | 0.01 | 0.01 | 0.01 | 0.01 | 0.01 | 0.01 |
| $\sigma_s$ | 0.96 | 0.99 | 0.98 | 0.88 | 0.85 | 0.80 | 0.77 | 0.75 |
| $\Delta\sigma_s$ | −0.03 | −0.01 | −0.03 | −0.02 | −0.01 | −0.04 | −0.02 | −0.03 |
| $\Delta Q/Q(\%)$ | 0.33 | 0.51 | 0.66 | 0.87 | 1.25 | 2.14 | 4.96 | 10.24 |
| $\Delta H_0/H_0(\%)$ | 0.22 | 0.32 | 0.51 | 0.66 | 0.89 | 1.52 | 2.69 | 15.24 |

typical section of the floodgate was measured by the pitot tube and the time-moving pointer bracket device. Figure 5 shows the comparison between the calculated value and the measured value of the vertical velocity in the typical section under the check condition of the spillway gate:

It can be seen from Fig. 5 that the test results are in good agreement with the calculated results in the trend, and the mathematical model can better reflect the variation law of the flow velocity of the flood gate, and the error between the two is small at the same section, which is in line with the actual situation.

## Outlet Flow of Gate Hole

Outlet flow of gate dam includes outlet flow of gate orifice and breast wall orifice, and its water flow condition is mainly affected by upper and lower boundary of orifice. The lower boundary of the orifice is generally a practical weir, a wide crest weir or a flat bottom (gate), while the upper boundary includes a flat gate, a radial gate, and the bottom edge of the breast wall [23, 24]. The bottom edge of breast wall is generally made into circular arc or elliptic curve in engineering. Therefore, the boundary conditions of the orifice can be summarized as different combinations of practical weir, wide crest weir, flat gate, flat gate, arc gate (breast wall), and elliptical breast wall; meanwhile, the submerged influence of downstream water level should be considered.

In this test, the orifice outflow of the cross-section model of the spillway gate of the orifice outflow dam is a combination of a wide-topped weir and a flat gate, and this combination is also very common in cascade channelization of the orifice outflow dam and many similar pivotal projects, so it is of great use value to study its discharge capacity [25].

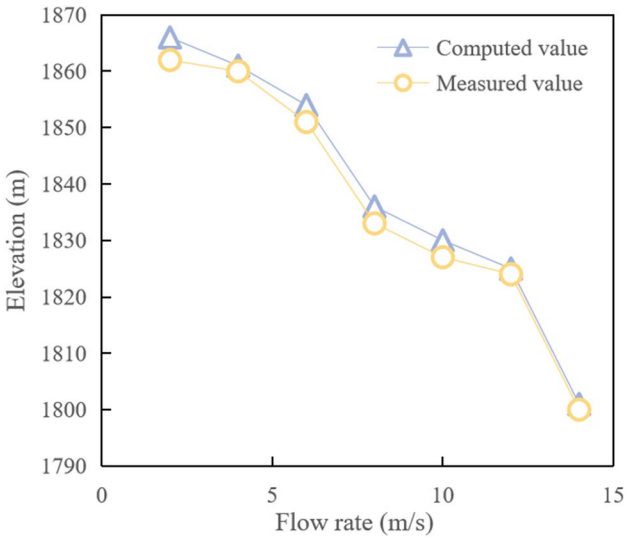


**Fig. 5** Velocity distribution of vertical line in typical section of spillway gate

(1) Experimental situation in this paper

$$Q = \mu eb\sqrt{2gH_0} \tag{12}$$

In which:

$$\mu = \varepsilon'\varphi\sqrt{1-\varepsilon'\left(e/H_0\right)} \tag{13}$$

In the above formula:

$\mu$ Flow coefficient of gate hole over current;
$e$ Opening of gate hole, m;
$b$ Width of gate hole, m;
$\varepsilon$' Vertical shrinkage coefficient.

In the calculation of gate outlet, the discharge coefficient $\mu$ of gate outlet is generally determined. Because $\mu$ is related to the form of gate sill, gate type, and relative opening $e/H$ of gate outlet, the calculation is complicated. In the calculation of practical projects, empirical formulas are generally used.

In this test, the outlet form of sluice gate is the combination of flat gate and wide-topped weir, and the empirical formulas for the free outlet flow coefficient of this combination are as follows [26]:

**Method 1:** The empirical formula of flow coefficient is:

$$\mu = 0.60 - 0.18(e/H) \tag{14}$$

The applicable range of relative opening is $0.1 < e/H < 0.65$.

**Method 2:** The formula form is:

$$\mu = 0.60 - 0.176(e/H) \tag{15}$$

**Method 3:** Sokonov formula: According to the test data of him and Leltov, the calculation formula of flow coefficient is as follows:

$$\mu_a = 0.62 - 0.074(e/H) \tag{16}$$

In the formula, $\mu_a$ is the discharge coefficient corresponding to the head above the midpoint of the hole and its relationship with $\mu$ is as follows:

$$\mu = \sqrt{1-e/\left(2H_0\right)}\mu_a \tag{17}$$

**Method 4:** The given flow coefficient formula is:

$$\mu_a = 0.352 - 0.264/\left[2.178(e/H)\right] \tag{18}$$

The applicable range of relative opening is $e/H = 0.05 \sim 0.68$.

In order to explore the outflow condition of the gate hole under different relative gate openings, in this test, the water level elevation of the upstream reservoir is kept at 328 m, and the free outflow under the sluice gate is determined by the needle reading of the water measuring weir under different relative openings [27, 28], and then the discharge coefficient $\mu$ is calculated by the following formula

$$\mu = Q/\left(eb\sqrt{2gH_0}\right) \tag{19}$$

Comparing the $\mu$ value of discharge coefficient measured by experiment with the calculated results of the above four methods and formulas, it is found that there are differences between the calculated values of the above four methods and formulas and the experimental values, as shown in Table 2. The analysis of the reasons may be related to the fact that each formula only reflects the linear relationship between the discharge coefficient and the relative opening, but the actual relationship between them is non-linear. When using the formula of East China Institute of Water Resources, the results are not ideal, which may be caused by different test conditions, so the calculation results are not listed in Table 2.

In order to reflect the actual situation of the project more accurately, so that it can be applied in similar projects, we processed the test flow coefficients under various relative openings in Table 2, regressed the test data by the principle of least square method, and deduced that there is a logarithmic distribution law with high correlation between the discharge coefficient $\mu$ of the gate hole and the relative opening $e/H$ of the gate, and its regression equation is:

$$\mu = 0.425 - 0.056ln\left(\frac{e}{H}\right) \tag{20}$$

The correlation coefficient between the discharge coefficient $\mu$ and the relative opening $e/H$ of the gate is as follows: $R = 0.981$.

The applicable scope of formula (20) is $e/H = 0.06 \sim 0.65$.

When the calculation results of formula (20) are listed in Table 2, it can be seen that the deviation is much smaller than other formulas, and the absolute value is all within 1%. The relationship between the calculation results of different formulas and the test values is plotted in Fig. 6, from which it can be seen that the empirical calculation formula (20) has better calculation accuracy and can be applied to the calculation of sluice discharge of similar sluice dams.

In this chapter, FLUENT software is used to simulate the steady flow of the flood gate of Pianqiao Hydropower Station. The calculation results show that the simulated calculated values of hydraulic parameters such as discharge, water surface line, pressure distribution, and velocity distribution of flood gate are in good agreement with the measured values of hydraulic model experiment. It is reasonable and feasible to use the standard $K$-ε turbulent flow model and VOF method to track the free water surface, especially that the calculation method using steady VOF method to

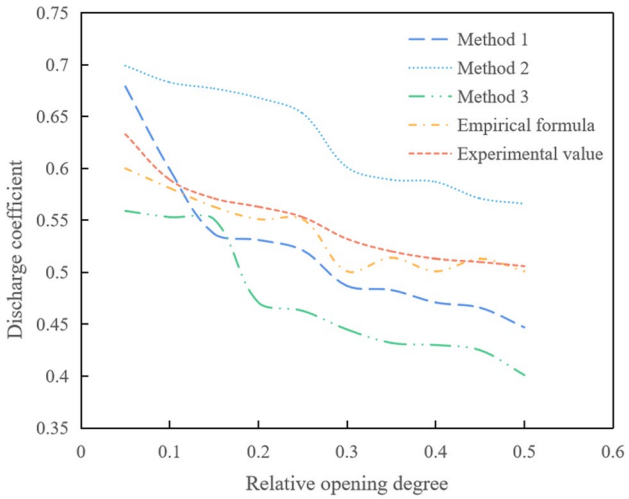


**Fig. 6** Comparison of calculation results of various formulas of flow coefficient $\mu$

**Table 2** Comparison of calculation results of outlet discharge coefficient $\mu$ of each formula

| Gate opening $e(m)$ | | 1.0 | 2.0 | 3.0 | 4.0 | 5.0 |
|---|---|---|---|---|---|---|
| Relative opening degree $e/H$ | | 0.062 | 0.122 | 0.174 | 0.221 | 0.302 |
| Experimental value $\mu$ | | 0.614 | 0.547 | 0.551 | 0.540 | 0.527 |
| Method 1 | Computed value | 0.554 | 0.560 | 0.553 | 0.520 | 0.511 |
| | Deviation% | −4.320 | −1.254 | 1.023 | 1.841 | 3.210 |
| Method 2 | Computed value | 0.561 | 0.552 | 0.533 | 0.526 | 0.517 |
| | Deviation% | −4.025 | −1.226 | 1.242 | 1.339 | 2.501 |
| Method 3 | Computed value | 0.669 | 0.524 | 0.517 | 0.503 | 0.479 |
| | Deviation% | −2.011 | 1.226 | 2.581 | 3.026 | 3.450 |
| Empirical formula (20) | Computed value | 0.663 | 0.564 | 0.552 | 0.531 | 0.510 |
| | Deviation% | 0.552 | −0.502 | 0.036 | −0.921 | 0.225 |

track the free water surface has high timeliness. To sum up, the numerical simulation data are in good agreement with the measured data of the model, which shows that the model used in numerical simulation is reasonable and the method is correct, which can provide a scientific and convenient way for the design and research of practical engineering.

## Conclusion

The problem of discharge capacity is an important issue related to whether or not to give full play to the benefits of the middle and low head sluice and dam hub and ensure the safety of the hub. Through model test and relevant theoretical analysis, this paper has made some discussions and studies on the discharge capacity and related parameters of the spillway gate of the orifice outflow dam and obtained some experimental and theoretical conclusions. The main aspects are summarized as follows:

(1) According to the experimental study, in the normal discharge range, the discharge coefficient $m$ of the flood gate hub increases with the increase of the upstream relative height difference $P_1/L$. It decreases with the increase of $d/L$. It increases with the increase of relative water heads $H_0/P$ and $H_0/d$. Through regression analysis, the empirical formula (20) considering discharge coefficient under different conditions is obtained, and it is verified that it can be applied to the calculation of discharge capacity of similar sluice-dam junction.
(2) When the water flow into the floodgate is asymmetric, it is easy to form a large vertical axis suction vortex in front of the floodgate, which leads to the decrease of the flow capacity. At the inlet of the orifice, the water flows quickly and is easy to escape. Affected by suction vortex and outflow, the water surface in the discharge tank fluctuates greatly.
(3) The results show that the discharge capacity of the spillway gate of the outlet dam mainly depends on the size of the head above the gate and the submergence degree below the gate. When the flood diversion level of the main stream is determined, controlling the submergence degree below the gate becomes the key to ensure the discharge capacity, which is closely related to the flood diversion channel in the flood storage and detention area.
(4) In the optimization scheme of this paper, increasing the radian of the side wall makes the water flow into the gate smooth and basically eliminates the vortex in front of the gate. At the same time, increasing the cross-sectional area of the orifice meets the requirements of over-flow and avoids the occurrence of off-flow, so that the water flow in the discharge tank is smooth and the water surface does not fluctuate. In view of the simplified body shape used in this paper, the over-flow capacity should be different from the actual project.

In this paper, the standard $K$-ε turbulence model is adopted, and the turbulent viscosity coefficient is an isotropic scalar, which cannot reflect the anisotropy of stress. In the future research, we can consider using other turbulence models to make up for this defect.

**Author Contribution** YXL and XSS designed research, performed research, analyzed data, and wrote the paper.

**Funding** This study is supported by construction and management of hydropower project open fund of Hubei key laboratory (No.: 2019KSD10).

**Data Availability** The data are available from the corresponding author.

**Code Availability** Not applicable.

## Declarations

**Conflict of Interest** The authors declare no competing interests.

## References

1. Shi CC, Wang ZZ, Peng Y (2020) Influence of relative difference between paired guide rails on motion accuracy in closed hydrostatic guideways. J Mech Sci Technol 34:631–648. https://doi.org/10.1007/s12206-020-0109-4
2. Thomidis T (2017) Influence of relative virulence and latent infections on the development of Monilinia to Greek peach orchards. Crop Prot 94:159–165. https://doi.org/10.1016/j.cropro.2016.12.001
3. Jin FB, Zhou YX, Bin L (2021) Influence of aging on creepage discharge characteristics of oil-paper insulation under AC-DC combined voltage. IEEE Access 9:49016–49024. https://doi.org/10.1109/ACCESS.2021.3064937
4. Khetarpal M, Singh S (2020) Relative influence of media and eWOM on purchase intention of green products. Int J Bus Global 26:407–416. https://doi.org/10.1504/IJBG.2020.111652
5. Birla S, Mondal DP, Das S, Kulshrestha A, Ahirwar SL, Chilla V, Kumar R (2019) Influence of cell anisotropy and relative density on compressive deformation responses of LM13-cenosphere hybrid foam. J Mater Eng Perform 28:1–11. https://doi.org/10.1007/s11665-018-3731-x
6. Chen CC (2017) The relative influence of travel favorability and importance on travel behavior. Tour Rev Int 21:395–405. https://doi.org/10.3727/154427217X15094520591367
7. Eddie D, Kelly JF (2017) How many or how much? Testing the relative influence of the number of social network risks versus the amount of time exposed to social network risks on post-treatment substance use. Drug Alcohol Depen 175:246–253. https://doi.org/10.1016/j.drugalcdep.2017.02.012
8. Shi JT, Zhu ZQ (2019) Influence of inner/outer stator pole ratio and relative position on electromagnetic performance of

partitioned stator switched flux permanent magnet machines. CES Trans Electr Mach Syst 3:259–268. https://doi.org/10.30941/CESTEMS.2019.00034
9. Hu Y, Xu Z, Li S, Yin Y, Jiang F, Liu S, Wu M, Yan C, Tan J, Yu G, Tong S (2019) Relative influence on childhood allergic diseases of meteorological factors and air pollutants in Shanghai. China Env Epid 3:398. https://doi.org/10.1097/01.EE9.0000610444.62187.c9
10. Dunn EC, Milliren CE, Evans CR, Subramanian SV, Richmond TK (2017) Disentangling the relative influence of schools and neighborhoods on A. Am J Public Health 105:e1–e9. https://doi.org/10.2105/AJPH.2014.302374
11. Behnia M, Wheatley C, Avolio A, Johnson B (2017) Influence of resting lung diffusion on exercise capacity in patients with COPD. BMC Pulm Med 17:1–9. https://doi.org/10.1016/j.chest.2016.08.991
12. Takaki K, Miura T, Oka A, Takahashi K (2020) Influence of relative humidity on ethylene removal using dielectric barrier discharge. IEEE T Plasma Sci 49:61–68. https://doi.org/10.1109/TPS.2020.3030800
13. Yuksek DA, Dumais SA, Kamo Y (2019) Trends in the relative influence of education and income on highbrow taste, 1982–2012. Sociol Inq 89:508–531. https://doi.org/10.1111/soin.12293
14. Godoy C, Thomas D (2020) Influence of relative humidity on HEPA filters during and after loading with soot particles. Aerosol Sci Tech 54:1–23. https://doi.org/10.1080/02786826.2020.1726278
15. Liu S, Tsona NT, Zhang Q, Jia L, Xu YF, Du L (2019) Influence of relative humidity on cyclohexene SOA formation from OH photooxidation. Chemosphere 231:478–486. https://doi.org/10.1016/j.chemosphere.2019.05.131
16. Harman RR, Leon A, Lancaster HM, Marshall JM (2019) Relative influence of spatial and structural characteristics of forest fragments on woody plant communities. Great Lakes Botan 58:32–44
17. Liu HY, Wang W, Hu CH, Xue WJ (2018) Calibration of discharge curve of flood gate based on relation curve and hydraulic method. Hydropower Autom Dam Monit 004(99–103):84
18. Li QM, Qiu Y, Wang SJ et al (2019) Study on the influence of side weir length change on the flow capacity of right-angle broken-line weir. J Hydraul Archit. Eng 1:177–181
19. Shu KF, Jing L, Fang J et al (2019) Numerical study on the influence of elbow angle on the flow capacity of water filling valve. Hydropower 045(100–103):119
20. Jin S, Li JQ (2020) Application of emergency control system of spillway gate in Zhentouba Hydropower Station. Autom Hydropower Plant 1:15–17
21. Zhu YX, Li ST, Yang F et al (2018) Numerical simulation study on flood discharge, energy dissipation and scour prevention of Chushandian Dam. Hydropower Energy Sci 036:132–135
22. Gu LZ, Zhao JK, Zhang XL et al (2020) Experimental study on discharge capacity of different types of gullies. Guangdong Water Resour Hydropower 292:21–25
23. Zhao HM, Qiu Y, Ma XH, Luo P, Li WZ (2017) Experimental study on flow capacity of W-shaped labyrinth weir. People's Pearl River 38:23–26
24. Hao X, Mu J, Shi H (2021) Experimental study on the inlet discharge capacity under different clogging conditions. Water 13(6):826
25. Shi Q, Wang W, Guo M et al (2020) The impact of flow discharge on the hydraulic characteristics of headcut erosion processes in the gully region of the Loess Plateau. Hydrol Process 34(3):718–729
26. Kwak J (2021) An assessment of dam operation considering flood and low-flow control in the Han River Basin. Water 13(5):733
27. Amon MR, Radi M, Staji Z et al (2021) Simplified indirect estimation of pump flow discharge: an example from Serbia. Water 13(6):796
28. Hojan M, Rurek M (2021) Effect of emergency water discharges from the dam in Wocawek on the sedimentary structures of channel bars in the lower flow regime of the River Vistula. Water 13(3):328